EXPERIMENTAL AND NUMERICAL SIMULATION OF THE BACKWARD EXTRUSION PROCESS FOR ANNEALED STEEL AISI 1010

Gilmar Cordeiro da Silva[1*], José Rubens Gonçalves Carneiro[1], André Bragança Carvalho França[1], Sara Aida Rodrígues Pulecio[2]

[1] Pontifícia Universidade Católica de Minas Gerais – Belo Horizonte – Minas Gerais – Brasil
[2] Universidad Del Valle Colombia
(*)*E-mail:* gilmarcord@gmail.com

RESUMO

Atualmente, apresenta-se como desafio a análise por elementos finitos e simulações de processos de conformar materiais. De um modo geral, a conformação requer vários estágios, e a sequencia de produção mais eficiente é obtida por intermédio de métodos empíricos através de experimentos e ajustes. A modelagem computacional de cada estágio do processo de conformação pelo método de elementos finitos aliado a existência de um banco de dados experimental pode tornar o projeto de fabricação mais rápido e eficiente, decrescendo os métodos de "tentativa e erros". Este trabalho avaliou as variáveis de processo no processo extrusão indireta do aço ABNT1010 recozido e trefilado utilizando experimentalmente matrizes fechadas e prensas hidráulicas. O pacote comercial utilizado na simulação da extrusão axissimétrica foi Deform 2D com as matrizes rígidas e o material elastoplástico. Correlacionou-se em uma das etapas do processo os resultados de nanodureza com a expressão analítica de Hollomon obtida no ensaio de tração. Com o uso da simulação numérica foi possível reduzir o número de estágios de fabricação, defeito de fabricação, prever a carga necessária e o perfil de deformação em cada estágio. A distribuição dos erros obtidos na simulação de carga através da técnica de elementos finitos e os experimentos apresentaram média de 11,76 e desvio padrão de 4,83 em razão da distribuição heterogênea de deformação.

Palavras-chave: *Simulação Numérica. Extrusão invertida. Nanoidentação. Método de elementos finitos.*

ABSTRACT

Currently it presents as a challenge the analysis of finite elements and simulation of processes of conforming materials. Generally, the conformation requires several stages, and more efficient production sequence is obtained by empirical methods through experiments and adjustments. Computer modeling of each stage of the conforming process of the finite element method combined with the existence of a database can make the experimental design for manufacture faster and more efficient, reducing the use of methods such as of "trial and error." This study evaluated the variables in the backward extrusion process and annealed steel AISI 1010 experimentally using closed dies and hydraulic presses. The commercial package utilized in the simulation of axisymmetric extrusion was Deform 2D, using rigid matrices and elastoplastic material. It was possible to correlate, in a stage, the results of nanohardness with the analytical expression of Hollomon obtained in the tensile test. Using the numerical simulation it was also possible to reduce the number of stages of manufacture, manufacturing defects, and to provide the required load profile at each stage of deformation. The distribution of errors obtained in the simulation load through finite element analysis and experiments showed a mean of 11.76 and standard deviation of 4.83 due to the heterogeneous distribution of deformation.

Keywords: *Numerical Simulation. Backward Extrusion Process. Nanoindentation. Finite element method.*

1. INTRODUCTION

Metal forming is a process widely used in manufacturing due to the minimal waste, dimensional accuracy and mechanical properties adjusted (Zhang et al. 2006). Extrusion is the process by which a block of material is reduced in cross section through its introduction in a hole under high pressure. Due to the high forces involved, most materials are extruded hot where resistance to deformation is low. The process of cold extrusion (direct and indirect) is possible for many materials and is an important alternative to business process. (Choi; Choi; Hwang, 2001; Farhoumand, 2009; Çan; Altinbalik; Akata, 2005).

The extrusion can be carried out either in hydraulic or mechanical presses. The mechanical presses are high productivity and high initial cost compared to hydraulic presses. Cold forming results in high production of pieces of low-cost material with excellent dimensional control and surface finish. Steels commonly used in cold forming of fasteners are low-carbon steels such as AISI 1010, replacing the machined steel AISI 12L14 and DIN 9SMn36 and low-alloy heat-treated AISI 10B22. All of these steels, except for AISI 1010 and AISI 10B22, are usually employed for the manufacture of electrical terminals in the machining process.

Computer modeling of each stage of the process of forming the finite element method can make the design of the sequence faster and more efficient, reducing the use of conventional methods of "trial and error" (Lima Roque; Button, 2000; Cho Et Al. 2003; Silva, 2011). The existence of a database obtained experimentally and in combination with specific forging simulation software enhances the value of the simulation, and more importantly, the development speed of the process. This work is therefore justified by the possibility that the finite element simulation provides to analyze the constraints of forging the parking brake terminal done in hydraulic press over the mechanical press of high-speed deformation. The cold forming has advantages over machining, such as material savings, productivity and operating cost.

This study used the numerical modeling via finite element (commercial software Deform 2D) and experimental methods in the manufacture of cold-extruded terminal hydraulic press, to enable the replacement of cold forming machining by optimizing the number of stages of operation.

2. EXPERIMETAL PROCEDURE

Chemical Analysis / Metallography and mechanical properties of raw material Figure 1 shows the dimensions of the terminal after cold extrusion. This terminal can be done by machining (AISI 12L14, DIN9SMn36, AISI 1010 (drawn wire) or 10B22 AISI (spheroidizing or quenched and tempered) or mechanical forming.

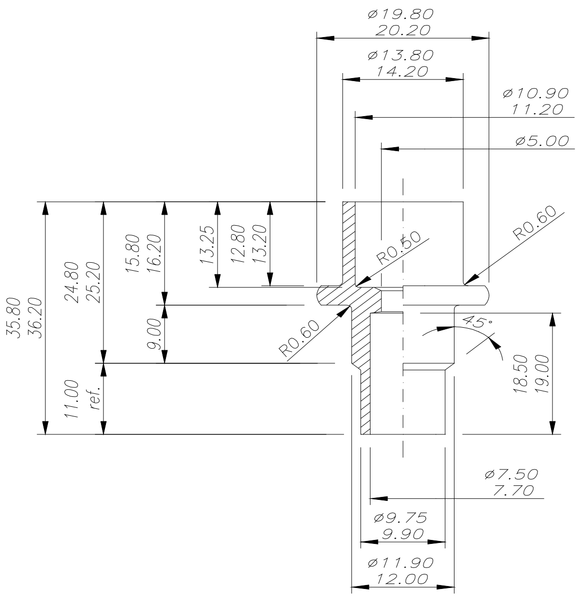

Fig. 1: Dimensions in mm of the terminals obtained after machining operation

The samples for chemical and metallographic analyses were cut perpendicular to the direction of lamination. These samples were milled and then polished with sandpaper in grit sizes 180, 240, 320, 400, 500, 600 and 1000 mesh. Then, finalizing of polishing was done with felt impregnated with diamond paste with dimensions 7, 3 and 1 μ. After finishing the polishing, the samples were analyzed without attack on an optical microscope, Leitz brand, an increase of 200X and scanning electron microscope, Jeol brand and voltage 20kV. To observe the microstructure, the samples were sprayed with 5% Nital.

Test of microhardness Vickers was done in microhardness instrument, Leitz brand, load of 100 gf for verification of mechanical properties. To obtain the stress-strain curves from instrumented indentation tests (EII), were cut 18 bar specimens with a diameter of 14 mm and length 3000 mm and drawn and annealed. The annealing treatment was done in a salt bath at temperatures of 900 ° C, heating time of one hour and cooling rate 100 ° C per hour, avoiding decarburization. The loads used for the instrumented indentation test were 10 mN, 40 mN and 70 mN and that led to the lowest standard deviation was 70 mN (0.05 GPa).

The bodies of the test piece of the wire rod diameter of 11.3 mm annealed were subjected to tensile test according to ASTM E-8M.

Four bodies were taken out of the test piece in the direction parallel to the lamination. The equipment used for the tensile test machine was an Instron universal TTDML, with servo-hydraulic load cell and 10 t. The strain rate was 0.2 cm / min. The value of the yield strength was obtained from the stress-strain graph from the deformation of 0.2%. An extensometer was used for the determination of the deformation in the direction of the body length of the test piece of 50 mm. After this deformation, the specimen was removed from the machine and measured, respectively, the final length and diameter.

The yield strength was calculated using Equation 1.

$$\sigma_R = \frac{Q_{MAX}}{S_0} \tag{1}$$

The value of the maximum load was reached in the peak load curve due to the variation of the initial length. Stretching was calculated by Equation 2

$$\Delta l = \frac{l_{ff} - l_0}{l_0} \tag{2}$$

where l_0 and l_{ff} are respectively the initial and final lengths.

The real deformation and stress are given by the Equations 3 and 4:

$$\bar{\varepsilon} = \ln(1+\varepsilon) \tag{3}$$

$$\sigma_r = \sigma(1+\varepsilon) \tag{4}$$

where ε is the conventional deformation, and it is given by the reason between the variation of the length and the initial length.

The resistance coefficient and strain hardening coefficient were calculated by the provision of 4 plastic parts of the region in a linear graph of Equation 5. (Garcia; Spim; Santos, 2000; Xinbo Et Al. 2002; Bergner; Zouhar, 2000)

$$\sigma_r = k \times \varepsilon^{-n} \tag{5}$$

where, σ_r and $\bar{\varepsilon}$ are respectively the real stresses and real strains.

3. NUMERICAL SIMULATION

The software used in the numerical simulation (commercial software DEFORMED 2D ® V-8,) consists of three modules, the pre-processor, the processor and post-processor, with the first and third modules in the same graphical environment.

The sequence of events for the simulation consisted of the input of variables such as materials Hollomon curve, coefficient of friction, speed, punch and definition of the initial pre-project concerning the initial geometry of the punches and matrices of each stage of the process (Silva, 2011; Santos Et Al. 2001).

The simulated initial pre-project involved cutting the billet and the initial five stages which are: calibration, first extrusion front, ahead of the second extrusion, extrusion and reversed repression (Fig. 2).

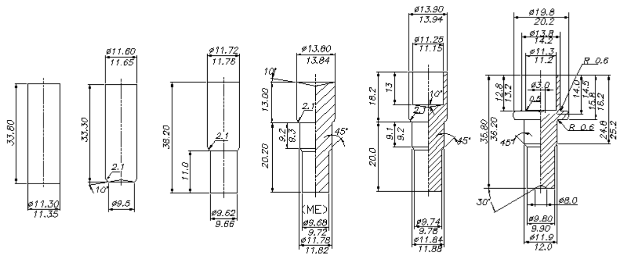

Fig. 2: Design of the six initial steps deemed necessary to produce the terminal.

The drawings of the dies and punches were inserted in the program submitted to boundary conditions and mesh generation followed by simulation. The play was considered rigid-plastic, while the tool is considered rigid (Schünemann; Ahmetoglu; Altan, 1996). Table 1 shows the process parameters used in the simulations of the extrusion.

Table 1: Values of parameters used in the simula**tion** of extrusion operations.

Material	AISI 1010
Punching speed (v)	11 mm/s
Coefficient of Friction (μ)	0,1
Temperature	25 °C
Stress- strain	obtained experimentally

The speed of the punch displacement was measured from the displacement of the cylinder of the press as a function of time. The time interval of each step of simulation was obtained by dividing the travel speed of the punch and the number of initial steps of 50. To pass the initial number of 50, there was a convergence of results for number of mesh elements between 400 to 2000 elements. The meshes were generated using the standard procedure of the program being used bi-linear isoparametric elements 4 knots. The coefficient of friction used was established according to the literature and constant throughout the simulation. (Schünemann; Ahmetoglu; Altan, 1996).

For numerical simulation of pre-project used the AISI 10B22 which was provided spheroidizing. It was found that it was possible the production of the dimensions of the project, using or not the first stage which is the calibration step. As well, this first stage was eliminated in the later stages of experimentation due to the load value found and obtain the product without this stage. There was also the appearance of folds in the sixth step simulation of material AISI 10B22. It was found in the numerical simulation that this bending is due to the depth of the extrusion with the repression reversed to obtain the flange. For the correction of this anomaly, the depth of the reversed extrusion of the fourth stage was reduced and the project was modified. The dimensional height of 13mm diameter was changed to a height of 10,5 mm (Machado, 2006). With this in later operation, there was formation of repression through the flange and this new sequence used for the simulation of physical materials annealed AISI 1010.

Based on the results obtained, the final design reduced the number of steps (Fig. 3).

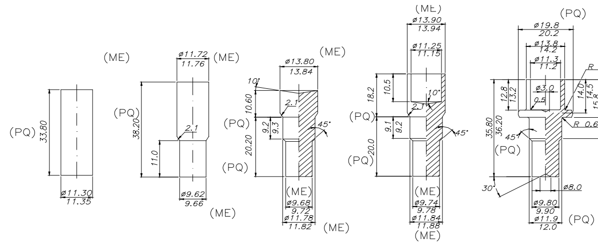

Fig. 3: Design of the final steps deemed necessary for the production of terminal.

The final sequence involved cutting the billet and the initial stages before the first extrusion, extrusion of the second front, inverted extrusion, extrusion and end repression.

For the final project were carried out experimental and numerical simulations with AISI 1010 steel. The results obtained in the post-processor loads were simulated for different stages of the project, which subsequently were compared with experimental loads obtained by physical simulation.

4. RESULTS AND DISCUSSION

Table 2 shows the chemical analysis of research material, in percent by weight.

Table 2: Chemical composition in percent by weight of the AISI 1010 steel used in the experiment.

STELL	AISI 1010
C	0,10
Mn	0,43
Si	0,10
P	0,021
S	0,009
Pb	0,00
Ti	0,001
Al	0,032
N(ppm)	33

The optical microscopy revealed the presence of ferrite and pearlite, in samples obtained according to the rolling direction in steels AISI 1010 (Fig. 4).

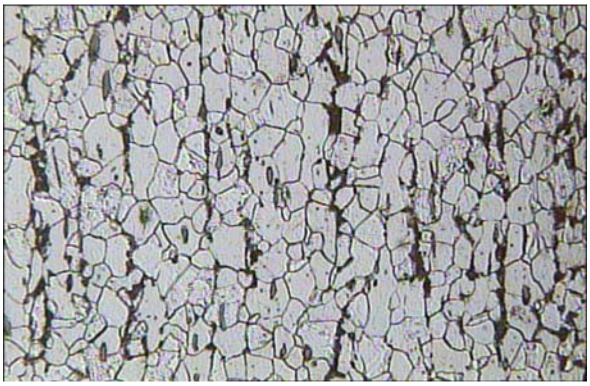

Fig. 4: Samples of the steel ANSI 1010. Attack Nital 5% and picrato of sodium; Increase 200X

Figure 5 shows the curve log (σ) versus log (ε) to the specimen steels AISI 1010.

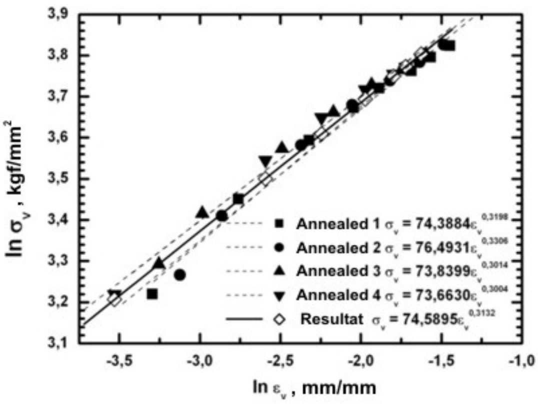

Fig. 5: Evolution of the ln true strain versus ln true stress of the steel annealed AISI 1010, obtained in the stress test with strain rate of 0.2 cm / min.

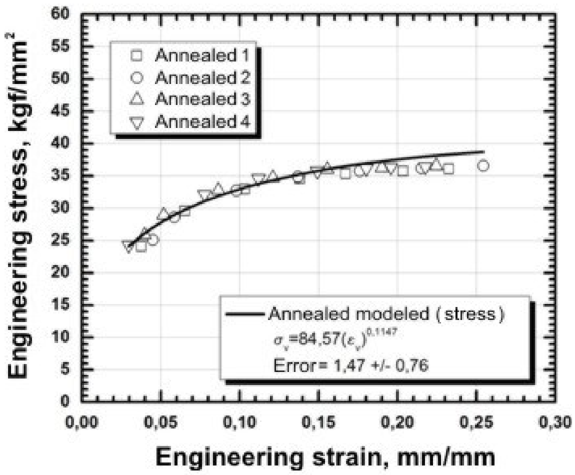

Fig. 6: Evolution of engineering deformation versus engineering strain modeled from the results of stress tests.

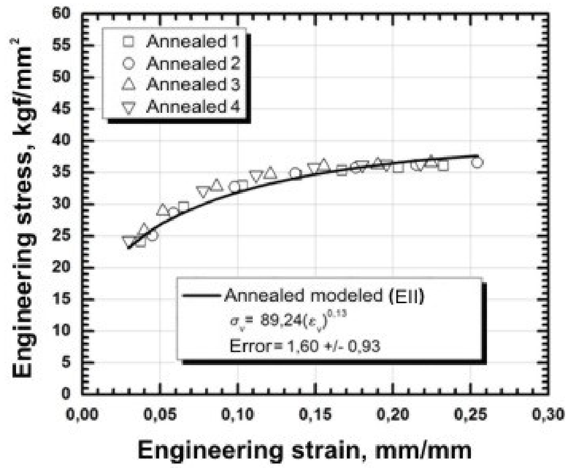

Fig. 7: Evolution of engineering deformation versus stress engineering modeled from the results of nanoindentation

From the data obtained was initiated numerical simulation for the AISI 1010 steel.

Figure 8 (a) shows the load versus displacement curve for the first extrusion step ahead of the material and AISI 1010 Figure 8 (b) shows the beginning and end of the simulation for the first stage. It is observed that the load moves up to 1000 kgf, stabilizes this value and then grows to 9000kgf. This stabilization 1000 kgf occurred due to compression of the material for the formation of the 9.62 mm diameter. The elevation of the load to 9000 kgf was due to the disposal of the material in the region of change of the diameter of 11 mm for the diameter of 9.62 mm. Note that the load remained constant after the flow of the material with the formation of a diameter of 9.62 mm.

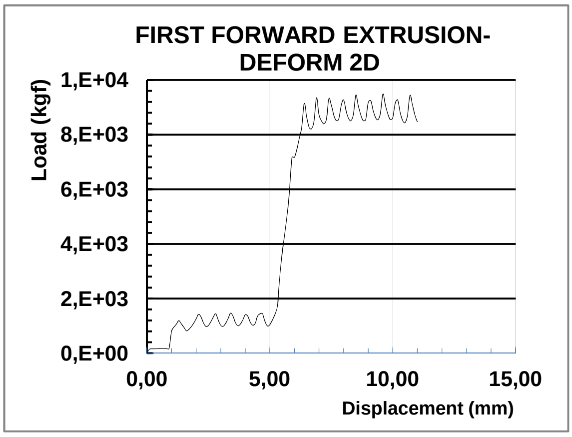

(a)

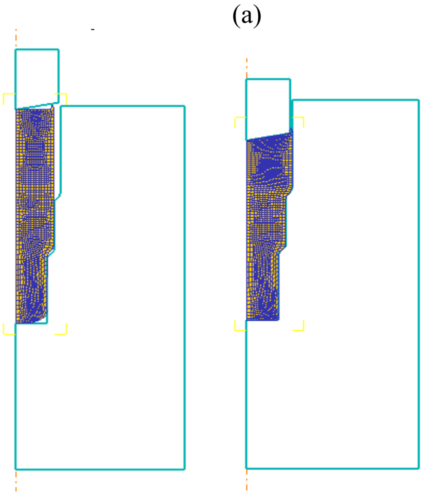

(b)

Fig. 8: Evolution of the load curve as a function of displacement (a) and start and end of the simulation for the first forward extrusion.

Figure 9 (a) and (b) shows the load versus displacement curve for the second extrusion step forward and start and end of the simulation of material AISI 1010. It appears that the initial displacement was 11 mm due to the conformation of the first operation is the basis for the second stage. At different stages of the simulation, we obtained the new mechanical properties in the program Deform 2D from the true stress-strain curve true original. In the range of displacement (11 to 15) mm there was an increase in load (0 to 1000) kgf due to compression set for the calibration of the diameters of 9.72 mm and 11.68 mm. Then, the load increased from 1000 to 6750 kgf for the formation of a diameter of 13.84 mm.

Figure 10 shows the geometry of the arrays, the specimen of test and of the punctures (0, 15, 20, 30 and 45 °) at the initial step and end of each simulation of the first stage of deformation.

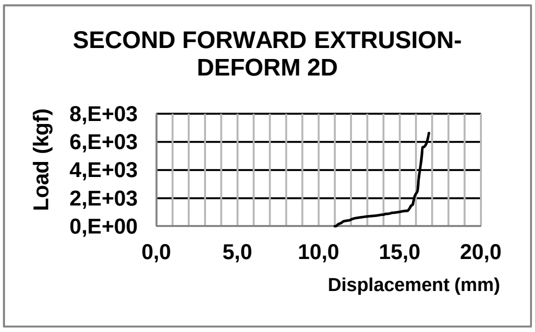

(a)

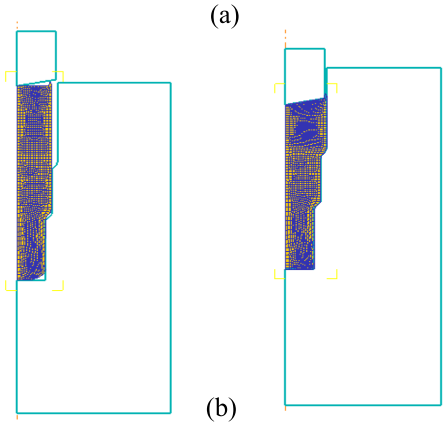

(b)

Fig. 9: Evolution of the load curve as a function of displacement (a) and start and end of the simulation for the second stage (b)

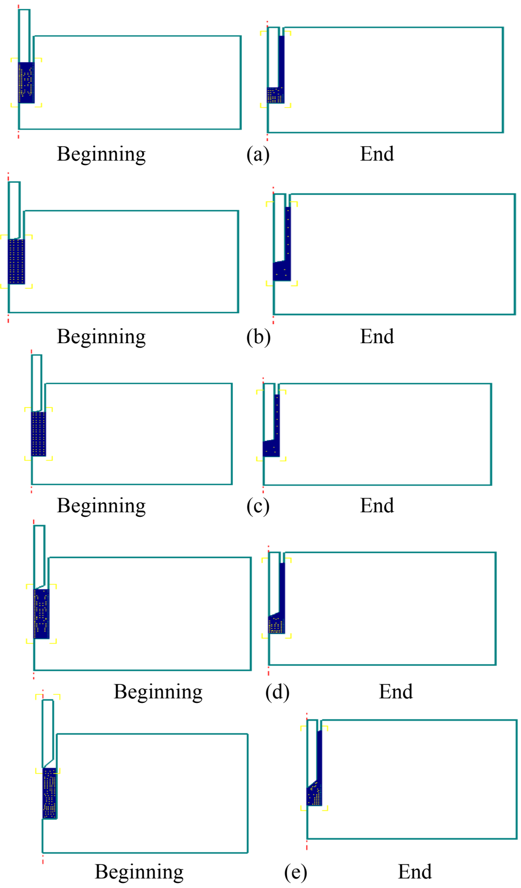

Fig. 10: (a) Punch 0°; (b) Punch 15°; (c) Punch 20°; (d) Punch 30°; (e) Punch 45°. All the punctures were the same course of displacement of 19 mm regardless of the angle.

The meshes with 170, 300, 500, 1000, 1500 and 2000 elements were initially assessed in the simulations. The mesh with 170 elements and 300 did not show convergence in the results for the load values in the extrusion reversed. Figure 11 shows the load values depending on the number of mesh elements and the puncture angle in which there was convergence in load values.

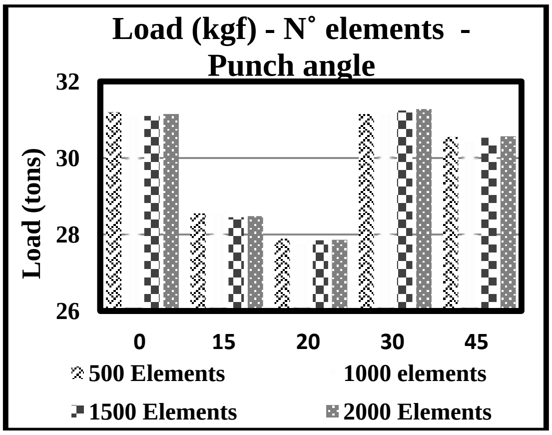

Fig. 11: Shipments (tones), sweaters and angles of the punctures

It can be observed that the lower load occurred in the simulations with the angle of the punch of 20°.

The mesh with 500 elements was chosen for the simulations due to convergence in the results and shorter processing times.

Figure 12 shows the behavior of load values (kgf) according to the angle of the puncture for the annealed material, obtained by numerical modeling and experimentally. In numerical simulations we used the curve obtained by tensile test and indentation.

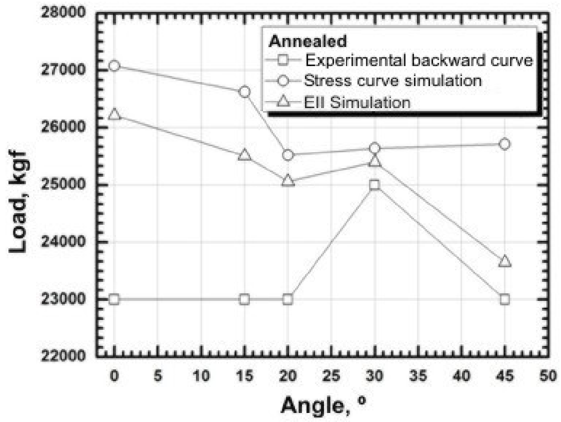

Fig. 12: Values of load (kgf) according to the angle of the punch.

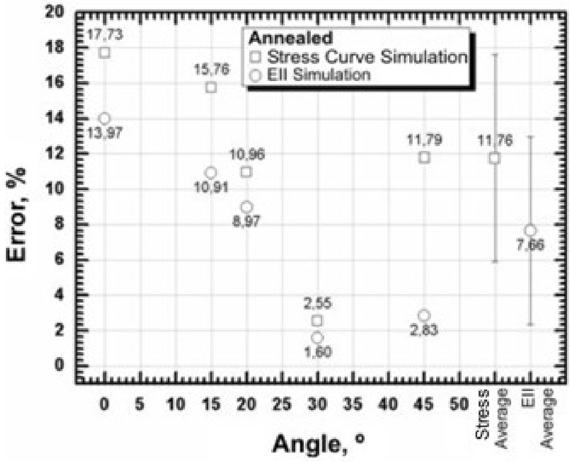

Fig. 13: Error loading of simulation.

The error of load of the simulation for the result obtained experimentally was calculated for different angles of punctures. Figure 13 shows these values of the error and also the values of the mean and standard deviation.

5. CONCLUSIONS

The method proposed by Bergner and Zouhar applied to the Paris equation allowed to obtain proper fit curve of Hollomon ;

The attainment of true strain curve versus true strain using the techniques of tensile test and instrumented indentation test give the same results without the need for correction proposed by some authors;

The distribution of load error between the finite element simulation and experimental results showed an average of 14.32 and 11.06 with standard deviation of 4.22 and 4.06 for the samples drawn.

6. REFERENCES

Bergner, F.; Zouhar, G.. A new approach to the correlation between the coefficient and the exponent in the power law equation of fatigue crack growth. International Journal of Fatigue, v. 22, p. 229-239, 2000.

Çan, Y.; Altinbalik, T. H.; Akata, E. A study of lateral extrusion of gear like elements and splines. Journal of Materials Processing Technology, v. 166, p. 128-134, 2005.

Cho, H.Y.; Min, G. S.; Jo, C.Y.; Kim, M.H. Process design of the cold forging of a billet by forward and backward extrusion. Journal of Materials Processing Technology, v. 135, p. 371-381, 2003.

Choi, H; Choi, J; Hwang, B. The forming characteristics of radial – backward extrusion - Journal of Materials Processing Technology, v 113, pp 141-147, 2001.

Garcia, A., Spim, J.A., Santos, C.A. Ensaios dos Materiais, 1ª ed., Livros Técnicos e Científicos Editora, Rio de Janeiro, 2000.

Farhoumand, R. E. Analysis of forward-backward-radial extrusion process. Materials and Design, v. 30, p. 2152-2157, 2009.

Lima Roque, C.M.O; Button, S.T. "Application of the Finite Element Method In Cold Forging Processes" , Journal of the Brazilian Society Mechanical Sciences, v XXII,n⁰ 2, pp 189-200, 2000.

Machado, A. Simulação Computacional para Fabricacão Terminal Elétrico. 2006 Monografia (Conclusão do Curso) Pontifícia Universidade Católica de Minas Gerais, Engenharia Mecânica, Belo Horizonte.

Santos, J.W.S., Muller, D., Glufke, L.A., Schaeffer, L., Recursos Informáticos Agilizam o Processo de Conformação, Revista Metalurgia e Materiais, p. 146-157, 2001.

Silva, G. C. Simulação numérica e experimental no processo de extrusão indireta a frio, considerando o efeito do caminho de deformação 2011. Tese (Doutorado Engenharia Mecânica) Pontifícia Universidade Católica de Minas Gerais, Belo Horizonte.

Schünemann, M., Ahmetoglu, M.A. Altan, T., "Prediction of Process Conditions in Drawing and Ironing of Cans", Journal of Materials Processing Technology, v 59, p 1-9, 1996.

Xinbo, L; Fubao, Z.; Jianhau, F.; Zhiliang, Z. Research on the flow stress characteristics of AISI 1006 and AISI 5140 in the temperature range of warm forging by means of thermo-mechanical experiments - Journal of Materials Processing Technology, v122, p. 38-44, 2002.

Zhang, X.Q.Peng, Y. H. Ruan, X. Y. Yamazaki, K. Feature based integrated intelligent sequence design for cold extrusion. Journal of Materials Processing Technology, v. 174, p. 4-81, 2006